Authors' response to Anonymous Referee #3:

We, the authors, are very thankful for the detailed and constructive comments and greatly appreciate the willingness to review our manuscript. Please find our responses below. The original comments are shown in **bold** with the respective answers below. Excerpts of the manuscript are shown in *italic writing*, whereas additions are written in blue and deleted parts in ~~red~~.
Please note that the format of citations in manuscript excerpts might be changed.
Thank you very much for your efforts,

Jannik Schottler on behalf of all authors

---

1)
The anonymous referee #2 has commented on the high induction factors and the choice of position of measurement plane, the different TI, Ct and blockage ratios for the two turbines tested, and the possible impact on the measured wake velocities. I understand that the wake effects are more easily studied at high induction factors, relatively close to the rotor, but I also share ref #2's curiosity about how this relates to real wind farms. I suggest a section showing the Ct vs. wind speed curve for a large modern wind turbine, and a few sentences about typical wind turbine spacings in recently built wind farms (along and across the main wind direction).

Thank you very much for this comment and the suggestions. The agreement with referee #2 shows that this is indeed an aspect that should be further elaborated on in the manuscript. We kindly ask you to refer to comment/answer #2 of referee #2, were we discussed the thrust coefficient, as well as comment/answer #5, where we discuss the choice of 6D and typical turbine spacings.

---

2)
The anonymous referee #1 main comment is on the impact of inflow velocity increments on the loads for a wind turbine. I would like to add a few comments on this topic. Figure 5 shows the mean velocity deficit at 6D behind the rotor. As expected, the wake (in terms of velocity deficit) has expanded somewhat, but at y/D and z/D of 1, we have more or less free stream conditions. Figure 6 shows the influence of the rotor in terms of TKE. Again we see that the wake has expanded, but at y/D and z/D of 1, we are almost at free-stream. Figure 7 is intriguing. Although the wake in terms of mean velocity deficit and TKE is hardly present at y/D and z/D of 1, the shape parameter here shows a strong signal, close to the maximum value across the measurement plane. My main comment is that the shape parameter can be high, but the velocity fluctuations may be too small to affect the loads. I therefore appreciate that the authors in the following figures try to present the results in different ways, but in my opinion, some more figures should be added here. In figure 8, the

probability density functions at the two points are normalized in different ways to be compared with the same Gauss distribution. What is the ratio of velocity increment standard deviations at the two positions? How would a plot look if the results were normalized in the same manner? In figure 9, the velocity increments at the two positions are again normalized with different standard deviations. I would like to see the corresponding plots also normalized with the standard deviation at D/2.

Thank you very much for this very constructive criticism and interest. I do understand that several questions are posed and details asked for in this comment. Nevertheless, I think it makes sense and adds clarity to answer the aspects mentioned in this comment in one answer as they are closely related. I will refer to specific aspects of the comment throughout the answer in bold writing.
To begin with, I think one has to pay attention to the term 'fluctuations'. Often in literature, fluctuations refer to

$$u'(t) = u(t) - \langle u(t) \rangle, \tag{1}$$

see equation 3 of the manuscript. When stating **'the shape parameter can be high, but the velocity fluctuations may be too small to affect the loads'**, we assume that not fluctuations in the sense of Eq. (1) but velocity increments are meant:

$$u_\tau(t) := u(t) - u(t+\tau), \tag{2}$$

which is statistically different as fluctuations are one-points quantities and increments two-point quantities. For a detailed elaboration we refer to Morales et al. [1].

'In figure 8, the probability density functions at the two points are normalized in different ways to be compared with the same Gauss distribution.'
This is not entirely correct and we want to clarify: the PDFs u_τ are indeed normalized by the standard deviation σ_τ and therewith by different values. This is not done to be compared to the same Gaussian. The normalization allows to purely compare the shape of the individual PDFs. The Gaussian is added to guide the eye as normally one is familiar with the Gaussian shape. As mentioned in the manuscript (p.14, ll. 14 ff), λ^2 is in indicator for a PDFs shape. Because of that, we normalize the PDFs in Fig. 8 to purely compare the shape and thus visualizing what is expressed by λ^2.
We fully agree and really appreciate the hint, that for a connection to loads, the absolute values of $u_\tau\,[ms^{-1}]$ are much more intuitive. However, we want to clearly distinguish this and order it the following way:

1. we find a ring of high λ^2 values (Fig. 7). This parameter expresses the *shape* of a pdf.

2. we show 2 exemplary increment PDF, normalized, in order to actually show the shape that is expressed by λ^2. We believe the shape is best compared by normalizing by the standard deviation

3. Fig. 10 shows that λ^2 is high where $\langle u \rangle$ would indicate free steam conditions

4. Now, we think it would be nice to show non-normalized plots, but comparing positions within the ring of high λ^2 values and the *free stream*. That way, we show much more intuitively that strong velocity jumps (increments) in short time scale happen significantly more often in the ring than in the free stream. Thus, we show that the ring is indeed no free stream as (falsely) suggested my defining a wake width by the velocity deficit in the wake. We show that is is significantly different regarding velocity increments, and therewith of importance.

For the above points 1. and 2., we think Fig. 7 and 8 should stay in the manuscript. Point 3. is expressed by Fig. 10. We suggest to add the following plots to bring across point 4.:
In order to comment on the impact on loads, or at least get a feeling for the potential impact, we agree that a non-normalized presentation is very beneficial. Figure 1 of this document shows the increment time series u_τ in free stream condition (a) and within the ring of high λ^2 values (b). One can clearly see that jumps exceeding 2.5m/s happen frequently in (b), and are non existent in the free stream. Hereby we show that this radial position of the wake features significantly different flows than the free stream. To show this more clearly, Figure 2 shows the corresponding increment PDFs, $p(u_\tau)$ of the absolute values. Clearly, one sees the same thing as in Fig. 1 (of this document):

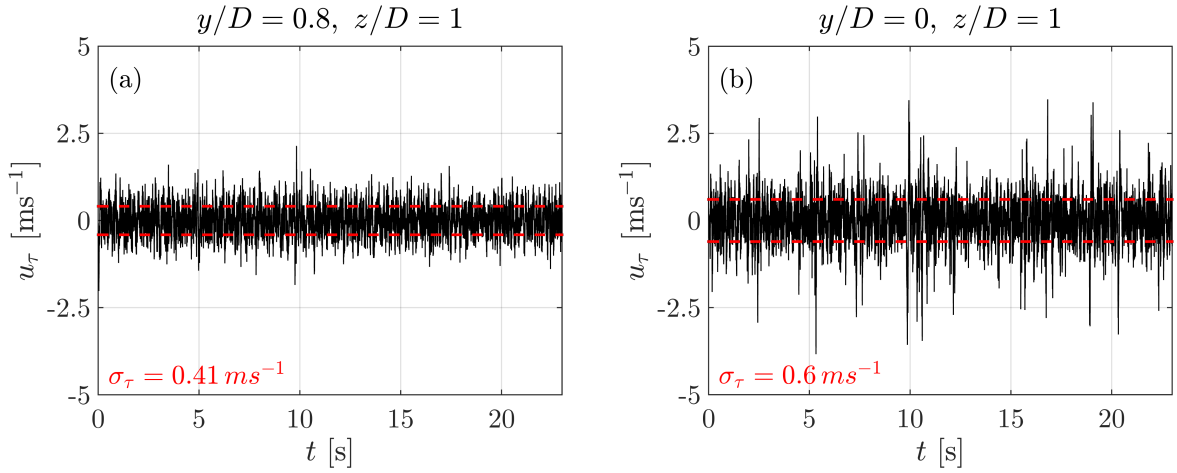

Figure 1. Time series of increments $u_\tau(t)$ for the positions $y/D = 0.8$, $z/D = 1$ (free stream,a) and $y/D = 0$, $z/D = 1$. The standard deviations σ_τ are indicated in red.

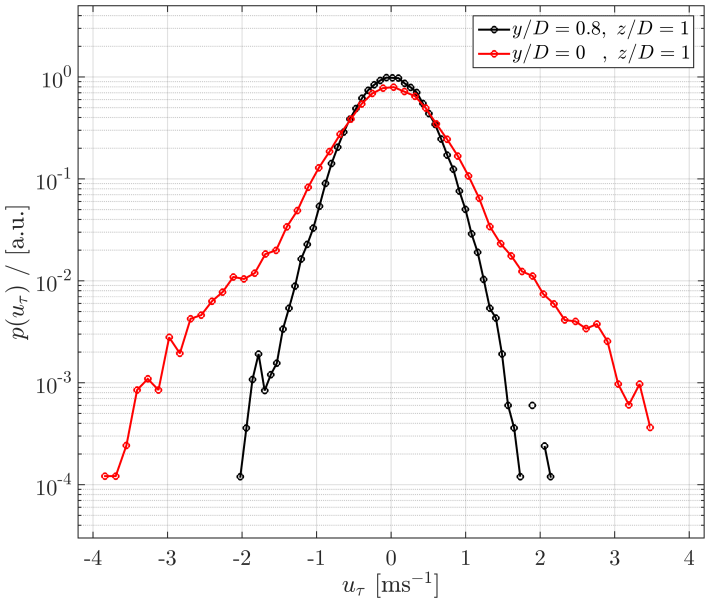

Figure 2. $p(u_\tau)$ of the free stream at $y/D = 0.8$, $z/D = 1$ and of $y/D = 0$, $z/D = 1$, exemplary for the ForWind turbine.

We suggest to update the Results-section of the manuscript the following way:

p.9 ll. 4 ff:
For $z = D$, which lies within the ring of large λ^2 values, $p(u_\tau)$ strongly deviates from a Gaussian, showing a heavy-tailed distribution ~~, indicating more frequent occurrences of extreme events. Exemplary, in both cases an event of $5\,\sigma_\tau$ is underestimated by multiple orders of magnitude comparing a Gaussian distribution to the PDFs at $z = D$~~. Figure 8 further shows $p(u_\tau)$ based on the model proposed by [2]. Those distributions were evaluated based on the λ^2 values computed by Equation (6) at $z = D$, visualizing exemplary how well the distributions' shapes are grasped by λ^2. ~~To show the difference in $p(u_\tau)$ more intuitively, Figure 9 shows the increment time series $u_\tau(t)/\sigma_\tau$ at $z = D/2$ and $z = D$, exemplary for the ForWind turbine. It can be seen how Figure 9(a) is characterized by noisy fluctuations while Figure 9(b) shows sudden jumps e.g. extreme events.$u_\tau(t)$ at $z = D/2$ (a) and $z = D$ (b) behind the ForWind turbine, cf. Figures 7(b) and 8(b). σ_τ is the standard deviation of u_τ.~~ Our results show that, depending on[...].

p.11, ll. 3ff:
*For illustration, the dotted lines in Figure 10 mark the respective locations. It is shown that the radial areas of TKE and λ^2 can be related in this way to the velocity deficit. To get a feeling of the impact on potential downstream turbine, Figure *2 of this response* compares $p(u_\tau)$ in absolute terms at a free stream position,$y/D = 0.8$, $z/D = 1$, and at a position featuring high λ^2 values, $y/D = 0$, $z/D = 1$, exemplary for the ForWind turbine. It becomes clear that velocity increments exceeding $3 ms^{-1}$ occur much more frequent within the ring of high λ^2 values than in three free stream. Hereby we show that this radial position of the wake features significantly different flows than the free stream. To compare more visually, Figure *1 of this response* shows the corresponding time series $u_\tau(t)$. Clearly, the spiky signature of extreme events become obvious in Figure*

1(b), confirming that no free stream condition is reached at $z/D = 1$.

p.14, ll.2 ff:
We find heavy-tailed distributions of velocity increments in a ring area surrounding *the velocity deficit and areas of high TKE in a wind turbine wake. Thus, the definition of a wake width strongly depends on the quantities taken into account as the ring area features significantly different statistics than the free stream. The heavy-tailed distributions are [...]*

We further suggest to delete Figure 9 of the manuscript. I think Figure 1 of this reply is more valuable and both might be a bit too much.

---

3)
Caption of Table 1, pg. 3: Is the effective velocity during turbine operation the relative wind speed with respect to the rotor tip? The blade tip of the ForWind turbine looks like it has a rounded shape. Where is the tip chord defined?

Thank you for pointing out that we should be a bit more precise here. As correctly described, the effective velocity vel_{eff} during operation is the wind speed the airfoil experiences at the tip. Indeed, the tip of the ForWind blades are somewhat round. To account for this we calculated the effective velocity and Reynolds number at $r \approx 96\%$ blade radius R and not at 100%. At $r = 0.96R$, the cord length is $c_{96\%} \approx 20mm$ and we can calculate the Reynolds number:

$$\omega = \lambda u / R \tag{3}$$
$$vel_{rot} = \omega r = \lambda u \cdot r/R \tag{4}$$
$$vel_{rot} = \lambda u \cdot 0.96 \tag{5}$$
$$vel_{eff} = \sqrt{u^2 + vel_{rot}^2} \tag{6}$$
$$vel_{eff} \approx 45.6 m/s. \tag{7}$$
$$\Rightarrow Re \approx 6.42 \times 10^4 \ . \tag{8}$$

I think it is still fair to call it Re_{tip} and suggest to clarify this in the updated manuscript by adding to the caption of Table 1:

p.3, Tab.1 (caption):
Summary of main turbine characteristics. The tip speed ratio (TSR) is based on the free stream velocity u_{ref} at hub height. The Reynolds number at the blade tip, Re_{tip}, is based on the chord length at the blade tip and the effective velocity during turbine operation. For the ForWind turbine, $0.96R$ was chosen as radial position to account for the rounded blade tips. The blockage corresponds to the ratio of the rotor's swept area to the wind tunnel's cross sectional area. The direction of rotation refers to observing the rotor from upstream, with (c)cw meaning (counter)clockwise. The thrust coefficients were measured at $\gamma = 0°$ and corrected for thrust on the tower and support structure.

---

4)
2.3, page 6: Please mention if measurements support the assumption about vertical vs transversal fluctuations. I assume you mean $\langle w^2 \rangle$ vs. $\langle w^2 \rangle$.

Thank you for this hint. In fact, we mean $\langle v'(t)^2 \rangle \approx \langle w'(t)^2 \rangle$ so the approximation of the TKE is satisfied:

$$k = 0.5 \left(\langle u'(t)^2 \rangle + \langle v'(t)^2 \rangle + \langle w'(t)^2 \rangle \right) \tag{9}$$
$$\approx 0.5 \left(\langle u'(t)^2 \rangle + 2\langle v'(t)^2 \rangle \right). \tag{10}$$

We did do measurements supporting this is a fair assumption. We suggest to add this information to the manuscript:

p.6, l. 6 ff:
For briefness, we write $\langle u \rangle$ instead of $\langle u(t) \rangle$. As the third flow component w was not recorded, we assume ~~$w'(t) \approx v'(t)$~~ $\langle w'(t)^2 \rangle \approx \langle v'(t)^2 \rangle$ so that Equation (2) becomes

$$k = 0.5 \left(\langle u'(t)^2 \rangle + 2\langle v'(t)^2 \rangle \right) \ , \tag{11}$$

which will be used in further analyses. Measurements where performed validating this approximation. For a thorough analysis[...]

---

5)
Caption, Figure 3: Consider adding something like: For the NTNU turbine, the wind tunnel walls are located at z/D = +-3.03 and y/D = +-2.02. For the ForWind turbine, the wind tunnel walls are located at z/D = +-4.67 and y/D = +- 3.12

We agree that this is helpful information and will add it as suggested in the updated manuscript. Thank you for the suggestion. We believe a factor 0.5 is missing in the suggested values, so we would like to edit the caption of Fig. 3 as follows:

p. 5, Fig 3(caption):
Non-dimensional measurement grid behind the rotor for $\gamma = 0°$. The respective contours of the turbines are shown in black (ForWind) and red (NTNU). For the NTNU turbine, the wind tunnel walls are located at $z/D = \pm 1.5$ and $y/D = \pm 1.0$, for the ForWind turbine at $z/D = \pm 2.34$ and $y/D = \pm 1.56$.

---

6)
Caption, Figure 11, pg. 12: Bottom row.

Thank you for this hint, it will be corrected.

---

7)
Caption, Figure 13: The red marks show the approximation of the respective parameter's radial extension based on $\mu \pm 1\sigma$ and $\mu \pm 2\sigma$ as described

in Section 3.1. But I see only two red lines, is it at one or two sigma?

Thank you for pointing this out. In the TKE contour plots (center column), the red lines correspond to $\mu \pm 1\sigma_\mu$ and in the λ^2 contours (right column), the red lines correspond to $\mu \pm 2\sigma_\mu$. We suggest to state this more clearly in the caption:

p.14, Fig 13, caption:
$\langle u \rangle / u_{ref}$ (left column), TKE (center column) and λ^2 (right column) for $\gamma = -30°$ behind the NTNU turbine (top row) and the ForWind turbine (bottom row). The time scale for λ^2 corresponds to the length scale of the rotor diameter. The red marks show the approximation of the respective parameter's radial extension based on $\mu \pm 1\sigma_u$ (TKE, middle column) and $\mu \pm 2\sigma_u$ (λ^2, left column) as described in Section3.1.

References

[1] Morales, A., Wächter, M., and Peinke, J., "Characterization of wind turbulence by higher-order statistics," *Wind Energy*, Vol. 15, No. 3, 2012, pp. 391–406.

[2] Castaing, B., Gagne, Y., and Hopfinger, E. J., "Velocity probability density functions of high Reynolds number turbulence," *Physica D: Nonlinear Phenomena*, Vol. 46, No. 2, 1990, pp. 177–200.